Natural Convection Heat and Mass Transfer in a Rectangular Porous Cavity Having Partially Thermally Active Walls

Rasoul Nikbakhti
Mashhad Aviation of Applied Science and Technology Training University, Mashhad, Iran
Email: rasoul.nikbakhti@gmail.com

Ahmad Saberi
Ferdowsi University of Mashhad, Faculty of Engineering, Mashhad, Iran
Email: ahmad.saberi@stu.um.ac.ir

***Abstract*—This study reports a numerical investigation of two-dimensional double-diffusive natural convection heat and mass transfer in a rectangular porous cavity with partially thermally active sidewalls. The length of the active part is equal to half of the cavity height. The top and bottom of the enclosure and inactive part of the sidewalls are assumed to be insulated and impermeable to mass transfer. The active part of the right sidewall has a lower temperature and concentration than the left one. The coupled differential equations are discretized by the finite difference method and are solved using the SOR method. The results are obtained for different active sections and different parameters such as aspect ratio and Darcy number. In addition, the heat and mass transfer rate in the cavity is measured in terms of the average Nusselt and Sherwood numbers.**

***Index Terms*—double-diffusive, rectangular cavity, porous medium, partially active walls, natural convection, heat and mass transfer**

I. Introduction

The problem of double diffusive natural convection in porous media has attracted considerable interest during the last few decades because of its wide range of applications, including grain storage and drying, oil and gas extraction, contaminant dispersion in underground water reservoirs, evaporative cooling of high temperature systems, spread of pollutants and many others. A comprehensive review of the literature concerning double-diffusive natural convection in a saturated porous media is presented in the book by Nield and Bejan [1]. An over view of the current state of the art of double diffusion in saturated porous media has been recently presented by Nield and Bejan [2] and Ingham and Pop [3] and [4]. Prasad and Kulacki [5] numerically investigated steady natural convection in a rectangular porous cavity. They found that the heat transfer rate increases as the aspect ratio is increased. An analytical and numerical study of natural convection heat and mass transfer through a vertical porous layer subjected to a concentration difference and a temperature difference in the horizontal direction has been studied by Trevisan and Bejan [6]. Double diffusive convection in a differentially heated cavity has been studied by Singh *et al*. [7]. They used the Brinkman– Forcheimer extended Darcy model for the momentum equations in the porous region. Chamkha and Al-Mudhaf [8] performed a significant Darcy–Brinkman investigation for double-diffusion natural convection flow in an inclined porous cavity. In general, the result showed that as the cavity inclination angle increases, reductions in the average Nusselt and Sherwood numbers were obtained. However, there was an exception at a critical angle, for which they achieved maximum values. Chamkha *et al*. [9] analyzed double-diffusive convection in an inclined porous enclosure with opposing temperature and concentration gradients. They found that the enclosure inclination angle strongly affected the average Nusselt and Sherwood numbers. Double diffusive natural convection in a square porous cavity submitted to cross gradients of heat and solute concentration has been numerically investigated by Bourich *et al*. [10]. Al-Farhany and Turan [11] analyzed numerically double diffusive natural convective heat and mass transfer in an inclined rectangular porous media. Two opposing walls of the cavity are maintained at fixed but different temperatures and concentrations while the other two walls are adiabatic. The results show that the average Nusselt and Sherwood numbers decrease when the angle of inclination increases. Muthtamilselvan and Das [12] have studied double diffusive natural convection of cold water around its density maximum in a two-dimensional enclosure filled with a water-saturated isotropic porous medium. It was found that the average Nusselt and Sherwood numbers showed nonlinear behaviors with increasing buoyancy ratio number.

In this paper, double-diffusive natural convection in a rectangular porous cavity filled with air and partially heated vertical walls for nine different heating sections is investigated. In fact the position of the partially active

Manuscript received July 1, 2015; revised October 21, 2015.

doi: 10.18178/ijmerr.5.1.72-76

sidewalls strongly affects the flow, heat and mass transfer characteristic and therefore the main objective of the present work is to determine in which combination we have the maximum rate of heat and mass transfer. In this respect, it is found the bottom-top active location is the most effective combination for heat and mass transfer rate in the enclosure.

II. Physical Modeland Governing Equations

The defined model is a two-dimensional rectangular porous cavity of height H and length L filled with moist air with Pr = 0.71, which is shown in Fig. 1. The partially thermally active sidewalls of the cavity are specified at two fixed different temperatures and concentrations. The left wall is partially at (T_h, C_h) and the right wall at (T_c, C_c) where (T_h> T_c) and (C_h> C_c), also the remaining sidewalls and horizontal walls are considered to be adiabatic. The length of the thermally active part is h = H/2. The heat and mass transfer characteristics are investigated for nine different combinations of the active walls. Placement order of thermal active section has significant influence on heat and mass transfer rate, to explore this effect and achieving the optimum rate inside the cavity, the following method is considered. The fluid is assumed incompressible, Newtonian, and viscous and the gravity acts in the downward direction. The viscous dissipation is assumed negligible.

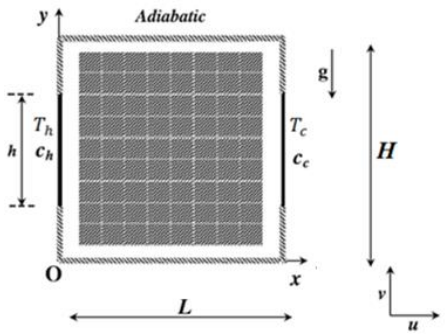

Figure 1. Physical configuration

The Boussinesq approximation with assisting thermal and solute buoyancy forces is used for the body force terms in the momentum equations, $\rho = \rho_0[1 - \beta_T(\mathrm{T} - \mathrm{T_c}) - \beta_C(\mathrm{C} - \mathrm{C}_c)]$ .With these descriptions and assumptions of the problem, and representing the position through Cartesian coordinate system in two dimensions, the governing equations could be written in non-dimensional form as the following:

$$\frac{1}{\varepsilon^2}\left[U\frac{\partial\xi}{\partial X}+V\frac{\partial\xi}{\partial Y}\right]=\frac{1}{\varepsilon}\left[\frac{\partial^2\xi}{\partial X^2}+\frac{1}{Ar^2}\frac{\partial^2\xi}{\partial Y^2}\right] + ArGr_T\left(\frac{\partial\theta}{\partial X}-N\frac{\partial S}{\partial X}\right)-\frac{1}{Ar}\frac{\xi}{Da} - \frac{1.75}{\sqrt{150}}\frac{\xi}{\varepsilon^{3/2}}\frac{\sqrt{U^2+Ar^2V^2}}{\sqrt{Da.Ar}} \quad (1)$$

$$-\xi = Ar^2\frac{\partial^2\Psi}{\partial X^2}+\frac{\partial^2\Psi}{\partial Y^2} \quad (2)$$

$$U\frac{\partial\theta}{\partial X}+V\frac{\partial\theta}{\partial Y}=\frac{1}{Pr}\left(\frac{\partial^2\theta}{\partial X^2}+\frac{1}{Ar^2}\frac{\partial^2\theta}{\partial Y^2}\right) \quad (3)$$

$$U\frac{\partial S}{\partial X}+V\frac{\partial S}{\partial Y}=\frac{1}{Sc}\left(\frac{\partial^2 S}{\partial X^2}+\frac{1}{Ar^2}\frac{\partial^2 S}{\partial Y^2}\right) \quad (4)$$

The boundary conditions in the dimensionless form are:

$$\theta = 0, S = 1, \Psi = \frac{\partial\Psi}{\partial Y} = 0$$

$$X = 0, M - \frac{1}{2} \le Y \le M + \frac{1}{2}$$

$$\theta = 0, S = 0, \Psi = \frac{\partial\Psi}{\partial Y} = 0 \quad :$$

$$X = 1, M - \frac{1}{2} \le Y \le M + \frac{1}{2}$$

$$\Psi = 0, \frac{\partial\theta}{\partial X} = \frac{\partial S}{\partial X} = 0 \quad :$$

$$X = 0,1,0 \le Y \le M - \frac{1}{2}, M + \frac{1}{2} \le Y \le 1$$

$$\Psi = \frac{\partial\Psi}{\partial X} = 0, \frac{\partial\theta}{\partial X} = \frac{\partial S}{\partial X} = 0 \quad :$$

$$0 \le X \le 1, Y = 0,1$$

where the non-dimensional variables and parameters are:

$$X = \frac{x}{L} \quad M = \frac{m}{H} \quad \xi = \frac{\omega}{\nu/_{HL}} \quad Gr = \frac{g\beta_T\Delta TL^3}{\nu^2}$$

$$Y = \frac{y}{H} \quad U = \frac{u}{\nu/_L} \quad \Psi = \frac{\psi}{\nu}\frac{L}{H} \quad \theta = \frac{T - T_c}{T_h - T_c}$$

$$Ar = \frac{H}{L} \quad V = \frac{v}{\nu/_L}\frac{L}{H} \quad N = \frac{\beta_C\Delta C}{\beta_T\Delta T} \quad S = \frac{C - C_c}{C_h - C_c}$$

$$Sc = \frac{\nu}{D} \quad Pr = \frac{\nu}{\alpha} \quad Da = \frac{k}{HL}$$

III. Method of Solution

Solution of the governing equations (1)–(4) together with the boundary conditions is performed numerically using finite difference method. The region of interest was covered with 'm' vertical and 'n' horizontal uniformly spaced grid lines. The transport processes, energy and mass equations are solved using the ADI (Alternating Direction Implicit) method and the stream function equation is solved by SOR (successive over-relaxation) method. The over relaxation parameter is chosen to be 1.8 for stream function solutions. The iteration is repeated until the convergence criterion $\frac{\Sigma_{i=1}^{m}\Sigma_{j=1}^{n}\left|\Phi_{i,j}^{k+1}-\Phi_{i,j}^{k}\right|}{|\Phi|_{max}\times m\times n} \ll 10^{-7}$ is satisfied for each variable. Where Φ stands for U, V, θ and S; k refers to time and i and j refer to space coordinates. The time step used in the computations is ranged between 0.00001 and 0.004 depending on Grashof number and mesh size.

IV. Results and Discussions

The results are presented in the form of streamlines, temperature and concentration distributions for nine different heating locations to show the fluid flow, heat and mass transfer phenomena in steady states. The flow patterns for different heating sections with following characteristics; Ar=2, Da=10^{-1}, Gr = 10^6, Le = 3, Pr=0.71,

ε = 0.35 and N= 0.2 are displayed in Fig. 2. In the first case, Fig. 2(a), both of heating sections have been placed on the upper sidewall of the cavity. Fig. 2(i) is mirror image of Fig. 2(a), which both of heating sections have been placed on the lower sidewall of the cavity. When heating sections are top–middle or middle–bottom, it can be seen that there is a principal cell which is situated near thermally active parts of the sidewalls whereas the remaining parts of the cavity maintained intact. When heating sections are top–bottom, a strange incident is occurred. It is observed that in Fig. 2(c) the current is in two distinct cells and the centre of each cell places in the near part of active thermally sidewalls. It is worthy to emphasize that in comparison with other sections, velocity and circulation rate of this section is in their minimum amount. In the next figure where the heating zone is located in the middle and the cooling one is on the top, (Fig. 2(d)), the principal cell almost occupies the whole cavity. In contrast, this case is responsible for a high rate of heat and mass transfer. Active section of bottom– middle (Fig. 2(h)) is mirror image of active section of middle–top (Fig. 2(d)). In Fig. 2(e) where both of heating sections placed in the middle sidewall of the cavity, the main strong cell is located in the central of the cavity and interestingly the flow pattern is completely symmetrical. In the bottom–top Fig. 2(g), the principle cell occupies the entire cavity. It is important to highlight that in this case, the rate of velocity and circulation accounts for the maximum.

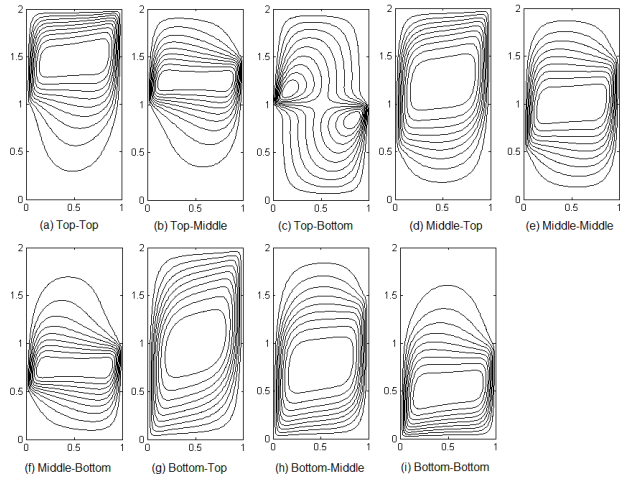

Figure 2. Streamlines for all heating sections, Ar=2, Da=10^{-1}, Gr = 10^{6}, Le= 3, N= 0.2.

Fig. 3 illustrates the temperature distribution inside the cavity for these cases by plotting the contours of isotherms. When the cooling section moves toward lower part of the enclosure (Fig. 3(c)), isotherms anticipate conduction in the middle of the cavity. In contrast to the other cases, in this combination the rate of heat transfer contributes to the least. Fig. 3(i) and (f) is illustration of mirror images of Fig. 3(a) and (b), respectively. In middle–top and bottom–middle active sections, a thermal boundary layer forms on the top and bottom part of cooling and heating sections, respectively, and convection is seen from isotherms of Fig. 3(h) and (d). Fig. 3(e) illustrates convection near the active sidewalls. In bottom–top active section, strong thermal boundary layers in the top part of cooling wall and bottom part of heating wall are formed shown in Fig. 3(g), in comparison to other sections in this case heat transfer rate has the largest share.

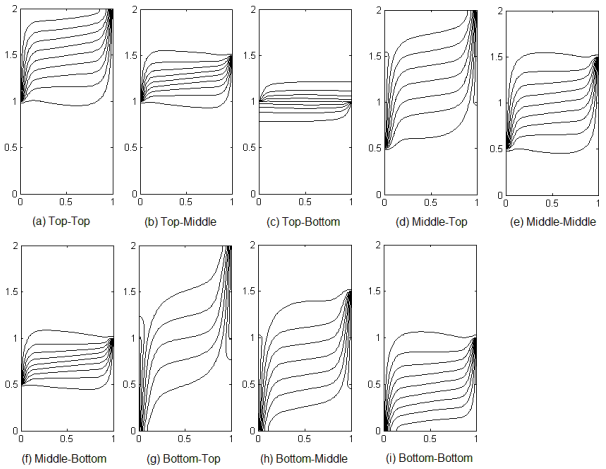

Figure 3. Isotherms for all heating sections, Ar=2, Da=10^{-1}, Gr = 10^{6}, Le= 3, N= 0.2.

Fig. 4(a–i) demonstrate the distribution of concentration. As it can be seen, the isopleths of concentration has similar behavior as that of temperature and this is mainly because of the similarity of energy equation and mass transfer equation. Based on Schmidt number which is greater than Prandtl number; the thermal diffusivity has greater effect on fluid than the mass diffusivity does. So, formed solutal boundary layer in Fig. 4(d) and (h), compared with formed thermal boundary layer in Fig. 3(d) and (h) is thinner. Strong solutal boundary layers are formed at the active sections, as seen in Fig. 4(g).

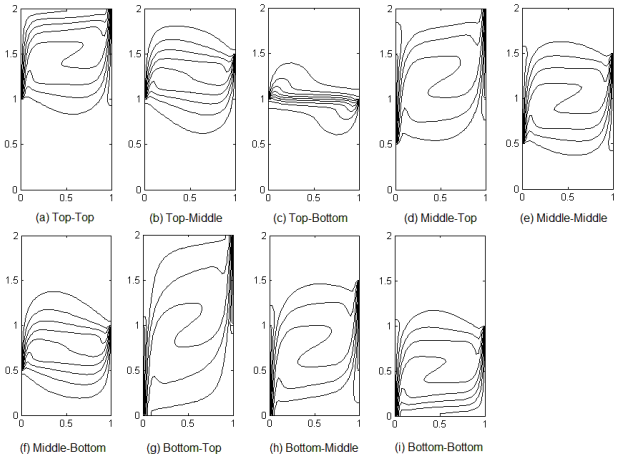

Figure 4. Isoconcentrations for all heating sections, Ar=2, Da=10-1, Gr = 106, Le= 3, N= 0.

Fig. 5 - Fig. 7 indicate the effect of Darcy number on the flow pattern inside the porous cavity for three different heating locations including top-bottom, middle-middle, and bottom-top. Darcy numbers are chosen as 10^{-8}, 10^{-5}, 10^{-3}, and 10^{-1}, in order to simulate the restricting

situations of Darcy flows. It is necessary to explain that for a low value of Darcy number ($Da \leq 10^{-5}$) a circulating flow pattern with the center of rotation at the middle of the cavity can be seen for all studied combinations of heating and cooling sections on the left and right walls respectively. That is, the fluid is moved upward near the partially heating wall and then downward near the cooling one. In the following, we take into account the influence of a high value of Darcy number for three mentioned combinations. In the first case, top–bottom active section, when Darcy number is 10^{-3} or 10^{-1} (Fig. 5(c, d)), two equal vortices are appeared near the thermally active sidewalls. This is mainly because in high Darcy numbers the fluid flow endures less resistance from the boundary friction, and flow is akin to pure buoyancy induced flow.

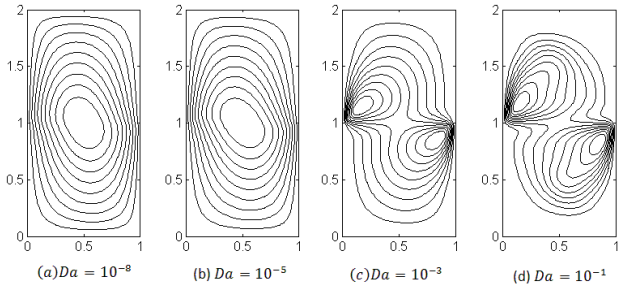

Figure 5. Streamlines for top - bottom heating location, Ar=2, N=1, Le=5, Ra=10^6.

In Fig. 6(c, d), both of heating sections have been placed in the middle sidewall of the cavity. In this case, there is a principal cell near the thermally active parts of the sidewalls.

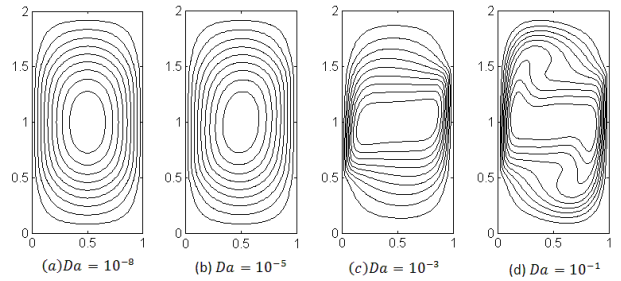

Figure 6. Streamlines for middle-middle heating location, Ar=2, N=1, Le=5, Ra=10^6.

In the bottom–top active section which is exhibited in Fig. 7(c, d) the clockwise principle cell occupies the entire cavity. Velocity and circulation rate in this case is a maximum. Furthermore, it can be seen from Fig. 5- Fig. 7 as Darcy number is increased from 10^{-5} to 10^{-3} then to 10^{-1}, the effects of viscous forces will be dominant so that the flow velocities are significant. As Darcy number is increased, the permeability of the porous medium rises and hence the boundary frictional resistance gradually reduces, in turn the fluid circulation is considerably improved within the cavity. Also, an increase in Brinkman term implies that the balance between Darcy term and the buoyancy force in the boundary layer is continuously replaced by the balance between a viscous force and the buoyancy force.

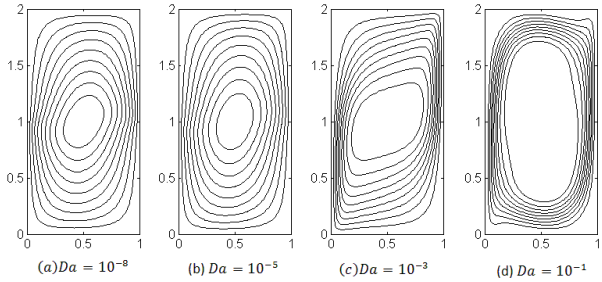

Figure 7. Streamlines for bottom-top heating location, Ar=2, N=1, Le=5, Ra=10^6.

The rate of heat and mass transfer in the enclosure is measured in terms of the average Nusselt and average Sherwood numbers. The average Nusselt and Sherwood numbers have been depicted in Fig. 8 as a function of Darcy number for different aspect ratios in bottom-top thermally active section in order to estimate how Darcy number affects the heat and mass transfer rate in the enclosure. It can be observed that from the graph, heat and mass transfer rate is considerably increased by increasing the aspect ratio. Also, the average heat and mass transfer rate increases by increasing Darcy number. This behavior is mainly due to the transition of the heat and mass transfer mechanism from conduction, low Darcy number, dominated flow to convection, high Darcy number. It is important to note that when $Da \leq 10^{-5}$, there is no any change occurred in the amount of the average Nusselt and Sherwood numbers however after which the average Nusselt and Sherwood numbers are suddenly surged by increasing Darcy number.

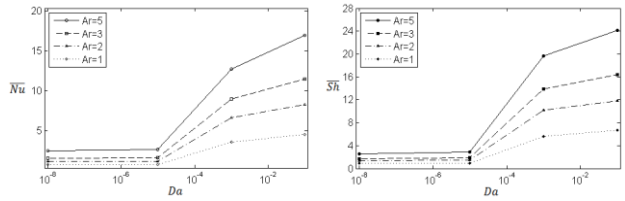

Figure 8. Average Nusselt and Sherwood numbers for different aspect ratio, Le = 3, Gr = 10^6.

V. Summary

Numerical study of double diffusive natural convection in a two-dimensional rectangular porous cavity has been investigated. The results are presented for different partially heating locations as well as Darcy numbers $10^{-8} \leq Da \leq 10^{-1}$ for some aspect ratios. The rate of heat and mass transfer in the cavity is high for the bottom–top thermally active section while it is poor in the top–bottom case. The heat and mass transfer rate are found to rise with increase in Darcy number as well as the aspect ratio.

Appendix List of Symbols

Alphabetics

Ar Aspect ratio
C Dimensional concentration (kg/m^3)
D Mass diffusivity (m^2/s)
Da Darcy number

g Acceleration of gravity (m/s^2)
Gr Grashof number
H Height of the cavity (m)
k Permeability of porous medium (m^2)
L Length of the cavity (m)
m Center of the heating section (m)
M Dimensionless of heating center
N Buoyancy ratio
Nu Local Nusselt number
$\overline{Nu}$ Average Nusselt number
P Pressure ($kg/m/s^2$)
Pr Prandtl number
S Dimensionless concentration
Sc Schmidt number
Sh Local Sherwood number
$\overline{Sh}$ Average Sherwood number
T Temperature (K)
u, v Velocity components (m/s)
U, V Dimensionless velosity components
x, y Dimensional cordinates (m)
X, Y Dimensionless coordinates

Greeksymbols

α Thermal diffusivity (m^2/s)
β_C Coefficient of concentration expansion(m^3/kg)
β_T Coefficient of thermal expansion (K^{-1})
ε Porosity
θ Dimensionless temperature
ν Kinematic viscosity (m^2/s)
ρ Density (kg/m^3)
ω Vorticity (s^{-1})
ξ Dimensionless vorticity
ψ Stream function (m^2/s)
Ψ Dimensionless stream function

Subscripts

c Cold wall and low concentration
h Hot wall and high concentration

REFERENCES

[1] D. A. Nield and A. Bejan, *Convection in Porous Media*, New York: Springer, 1992.
[2] D. A. Nield and A. Bejan, *Convection in Porous Media [Electronic Resource]*, Third ed., New York: Springer Science-Business Media, Inc. digital, 2006.
[3] D. B. Ingham and I. Pop, *Transport Phenomena in Porous Media*, Oxford: Elsevier, 2005, vol. 3.
[4] D. B. Ingham and I. Pop, *Transport Phenomenon in Porous Media*, Oxford: Pergamon, 1998, vol. 1.
[5] V. Prasad and F. A. Kulacki, "Convective heat transfer in a rectangular porous cavity – effect of aspect ratio on flow structure and heat transfer," *J. Heat Transfer*, vol. 106, pp. 158–165, 1984.
[6] O. V. Trevisan and A. Bejan, "Natural convection with combined heat and mass transfer buoyancy effects in a porous medium," *International Journal of Heat and Mass Transfer*, vol. 28, pp. 1597–1611, 1985.
[7] A. K. Singh., T. Paul, and G. R. Thorpe, "Natural convection due to heat and mass transfer in a composite system," *Heat Mass Transfer*, vol. 35, pp. 39–48, 1999.
[8] A. J. Chamkha and A. Al-Mudhaf, "Double-diffusive natural convection in inclined porous cavities with various aspect ratios and temperature-dependent heat source or sink," *Heat and Mass Transfer/Waermeund Stoffuebertragung*, vol. 44, no. 6, pp. 679–693, 2008.
[9] A. J. Chamkha and H. Al-Naser, "Double-diffusive convection in an inclined porous enclosure with opposing temperature and concentration gradients," *Int. J. Therm. Sci*., vol. 40, pp. 227-244, 2001.
[10] M. Bourich, A. Amahmid, and M. Hasnaoui, "Double diffusive convection in a porous enclosure submitted to cross gradients of temperature and concentration," *Energy Conversion and Management*, vol. 45, pp. 1655–1670, 2004.
[11] K. Al-Farhany and A. Turan, "Numerical study of double diffusive natural convective heat and mass transfer in an inclined rectangular cavity filled with porous medium," *Int. Communications in Heat Mass Transfer*, vol. 39, pp. 174–181, 2012.
[12] M. Muthtamilselvan and M. K. Das, "Double diffusive convection in a porous cavity near its density maximum," *Journal of Porous Media*, vol. 15, pp. 765-774, 2012.

Rasoul Nikbakhti was born in Mashhad in 1984. Nikbakhti is a MSc. Graduate in Mechanical Engineering (Energy Conversion) at Ferdowsi University of Mashhad, in Iran in 2010.
He has worked in Shargh Cement Complex as a MECHANICAL ENGINEER for 2 years. Now he is working as a LECTURER in the field of Mechanical engineering in Applied Science and Technology University. He has published some international journal and conference papers in Elsevier and ISME. His main research interests include analyzing heat and mass transfer phenomenon in porous media and now he is working on Improved Oil Recovery and Formation Damage in petroleum industry.
Mr. Nikbakhti is one of the members of Iranian Society of Mechanical Engineers as well as a member of Iranian Engineering Organization Province of Khorasan Razavi. He was awarded by Ferdowsi University because of publishing two international papers in 2012.

Ahmad Saberi was born in Mashhad in 1986. Now, Saberi is a P.h.D student in Mechanical Engineering (Energy Conversion) at Ferdowsi University of Mashhad, in Iran.
He has worked in Omran Gostaresh Company as a MECHANICAL ENGINEER for 5 years. Now he is working as a LECTURER in the field of Mechanical engineering in Ferdowsi University, Mashhad, Iran. He published several articles in the fields of heat transfer and two-phase flow. His main research interests include analyzing heat and mass transfer phenomenon in porous media, multi-phase flow, and now he is working on Nucleation phenomena in high-pressure steam flow.
Mr. Saberi is one of the members of Iranian Engineering Organization Province of Khorasan Razavi.